Operational Characteristics of Superconducting Amplifier using Vortex Flux Flow

Sung-Hun Lim[a]
Electrical Engineering, Soongsil University,
511 Sangdo-dong, Dongjak-gu, Seoul 156-743, Korea

[a]E-mail : superlsh73@ssu.ac.kr

(Received October 15 2008, Accepted December 11 2008)

The operational characteristics of superconducting amplifier using vortex flux flow were analyzed from an equivalent circuit in which its current-voltage characteristics for the vortex motion in YBCO microbridge were reflected. For the analysis of operation as an amplifier, dc bias operational point for the superconducting amplifier is determined and then ac operational characteristics for the designed superconducting amplifier were investigated. The variation of transresistance, which describes the operational characteristics of superconducting amplifier, was estimated with respect to conditions of dc bias. The current and the voltage gains, which can be derived from the circuit for small signal analysis, were calculated at each operational point and compared with the results obtained from the numerical analysis for the small signal circuit. From our paper, the characteristics of amplification for superconducting flux flow transistor (SFFT) could be confirmed. The development of the superconducting amplifier applicable to various devices is expected.

Keywords : Superconducting amplifier, Vortex flux flow, Vortex motion, Transresistance, Superconducting flux flow transistor(SFFT)

1. INTRODUCTION

Superconducting flux flow transistors(SFFTs) based on the control of the Abrikosov vortex flow across a weak link are the active devices using high-Tc superconducting thin films. Attractions of SFFT such as simple fabrication process using single layer film, lower threshold voltage and lower power loss have led a possibility for various applications of SFFT' devices[1-3].

However, most of researches have been devoted to analysis for the physical mechanisms of vortex flow caused by the application of a magnetic field, not to application of devices[4-7]. For the analysis of the physical operation of SFFTs, it is important to draw a model to describe the physical operation considering the current-voltage characteristics of SFFTs caused by the magnetic field, which is induced by the control current. Especially, for the circuit design of SFFTs to operate as an amplifier, the circuit parameters to affect the operating point have to be considered.

In this paper, the transresistance was derived from the induced voltage across the weak link by reflecting the effect of magnetic field induced by the control current. From an equivalent circuit including the transresistance, which is the important parameter to describe the transfer characteristics of SFFTs, the operating point of SFFTs was determined. Current and voltage gains of SFFT were calculated at each operational point, which is determined from the equivalent circuit connecting with a load terminal. The design conditions to increase two gain values of SFFT were also discussed.

2. DEVICE STRUCTURE AND MODELIZATION

SFFTs consist of a control line for generation of vortices in a channel and a body line with the channel. The thickness of the channel can be controlled by eching techniques as shown in Fig. 1. The magnetic field generated by the control current induces the vortices into the channel. The driving vortices by the Lorentz force cause an induced voltage in the body line. The induced voltage at the channel terminals of the body line, if a uniform magnetic field, B, is applied to the channel plane perpendicularly, can be derived as follows[8] :

$$V_O(B,I_B,T)=\left[\frac{\mu_O t\cdot v_{L_O} e^{-(E_P/k_BT)}}{d}\right]\cdot\left[I_B-\left(I_{CR}-\frac{2dB}{\mu_O}\right)\right], \quad (1)$$
$$\times\sinh\left[\frac{I_B}{(wk_BT/\delta\phi_O)}\right]$$

where E_P is the pinning energy, k_B Boltzman's constant, $\emptyset_0$ the flux quantum, δ the pinning potential range, V_{Lo} the maximum vortex velocity along the edges of the flux channel and μ_0 permeability of vacuum. t, d and T are the width of the channel, the thickness of the channel and temperature, respectively. I_{CR} is the critical current of the channel.

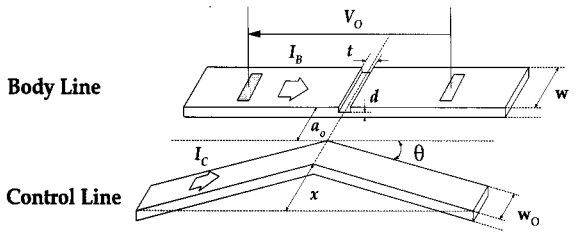

Fig. 1. Schematic structure of the superconducting flux flow transistor with a single channel.

In the equation (1), the magnetic field density at the center of the channel of the body line can be derived from the Biot-Savart's law as follows:

$$B(I_C)=\left[\frac{\mu_O\sin\theta\cdot I_C}{2\pi(x+w_O/2+a_O+w/2)}\right] \quad (2)$$
$$\times\left[\sin\left\{\tan^{-1}\left(\frac{x\tan\theta}{x+w_O/2+a_O+w/2}\right)\right\}\right]$$

where x and a_o are a distance from inner edge center of the control line to the center of straight line connecting both sides of the edge of the control line and the distance between the control line and the body line, respectively. w_o and w are the widths of the control line and the body line, respectively. θ is the angle between the control line and the center line as shown in Fig. 1.

The induced voltage considering the magnetic effect by the control current can be obtained by substituting magnetic field intensity of equation (2) for B in the equation (1), which is suggested by us. The current-voltage characteristics of SFFTs are shown in Fig. 2. The specifications of the superconducting flux flow transistor with the designed single channel are listed in Table 1.

In the equation (1), to reflect the dependence for the control current in case that the body current does not excess the critical current of the channel, the critical current of the channel, I_{CR}, is replaced with the equation (3) as follows:

$$I_{CR} = I_{CRO} - \alpha I_C \quad (3)$$

where α is fit parameter and I_{CRO} is critical current of the body line in case that the control current does not flow.

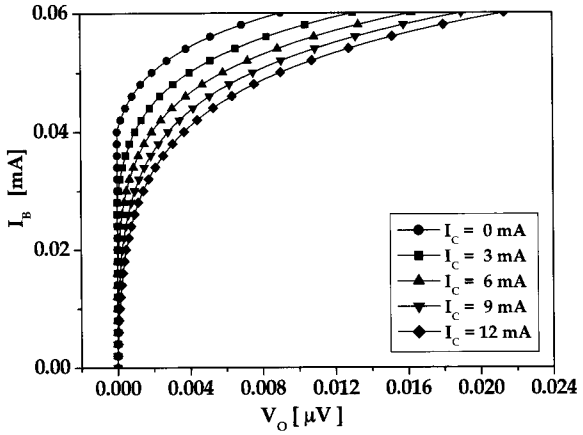

Fig. 2. Current-voltage characteristic curves of SFFT.

Table 1. Specifications of the superconducting flux flow transistor with a single channel.

	Parameters	Value
t	Width of channel	3 μm
d	Thickness of channel	0.4 μm
w	Width of body line	50 μm
a_O	Distance between control line and body line	5 μm
x	Distance from inner edge center of control line to center of straight line connecting both side edge of control line	185 μm
w_O	Width of control line	20 μm
θ	Angle between control line and center line	3/π rad

The temperature around the channel, which is included in the equation (1), is changed linearly from temperature of liquid nitrogen to critical temperature of $YBa_2Cu_3O_X$ with the control current.

The gain of SFFT or the transresistance r_m, which is defined as the ratio of the voltage change in the output terminal to the change of the applied control current, is calculated from the equation (1). Figure 3 shows the results. As the body current increases, the transresistance increases but the control current corresponding the occurrence point of r_m decreases, which results from the appearance of enough vortex flow within the channel to induce the voltage across the channel.

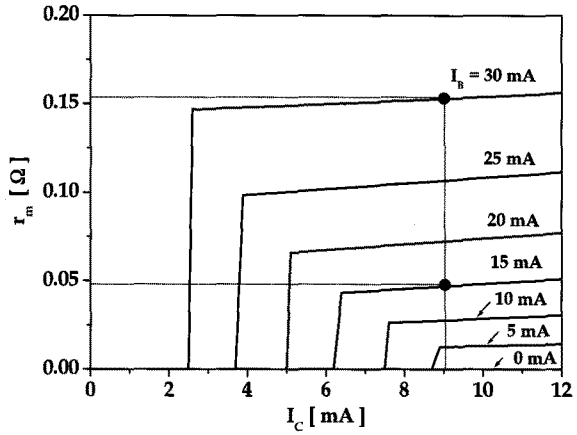

Fig. 3. Control current dependence of transresistance calculated from current-voltage characteristic curves of SFFT.

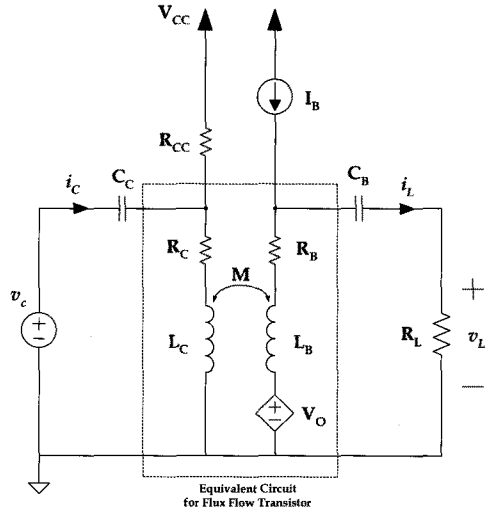

Fig. 4. Conceptual circuit to illustrate the operation of the SFFT as an amplifier.

The conceptual circuit to illustrate the operation of SFFT as an amplifier is shown in Fig. 4. The capacitor C_B and C_C are coupling capacitors whose purpose is to couple the signal V_C to the control line and the load R_L to the body line, respectively. L_C, L_B, R_C and R_B represent the inductance and the resistance of both the body line and the control line including each contact resistance. M is the mutual inductance between the control line and the body line. In the analysis for low frequency operation, L_C, L_B and M can be ignored for simplicity. The analysis for the circuit is divided ino two steps, dc bias analysis and small signal analysis. In the dc bias analysis, the operating point can be determined with $V_C = 0$. Assuming $R_C = R_B = 0.02\ \Omega$, $R_L = 0.04\ \Omega$, $L_C = L_B = 10$ pH and M = 0.5, the dc current for each line, I_C and I_B and the induced voltage across the channel terminals of the body line, V_O can be determined from adjustment of V_{CC}, R_{CC} and I_B, which fixes the operating point of SFFT and the transresistance as shown in Fig. 2 and 3.

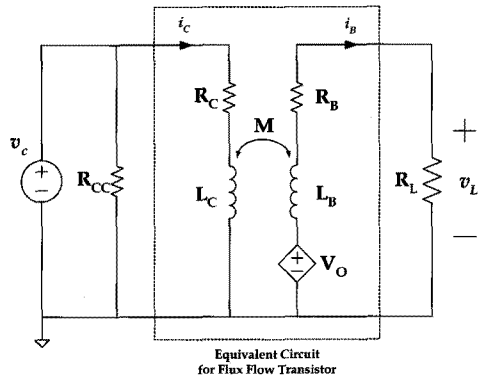

Fig. 5. Circuit for small signal analysis as the amplifier of SFFT.

From the circuit for small signal analysis shown in Fig. 5, the circuit equation is described as the equation (4) assuming that R_{CC} is high.

$$\begin{bmatrix} v_C \\ 0 \end{bmatrix} = \begin{bmatrix} R_C & 0 \\ -r_m & R_B + R_L \end{bmatrix} \begin{bmatrix} i_C \\ i_B \end{bmatrix} + \begin{bmatrix} L_C & -M \\ -M & L_B \end{bmatrix} \begin{bmatrix} \dot{i}_C \\ \dot{i}_B \end{bmatrix} \quad (4)$$

Applying the numerical analysis, for example, FDM (finite dimension method) into the equation (4), the variance of currents of the control line and the body line at each time step can be obtained.

3. SIMULATION RESULTS FOR MODEL

The simulated waveforms for the voltage across the channel (v_O) including the voltage in the load (v_L) and current at the control line (i_C) and the body line (i_B) are shown in Fig. 6. Voltage and current gains, which can be derived from Fig. 5, were calculated. In case that V_{CC}, R_{CC} and I_B are 9 V, 1 kΩ and 15 mA, the current gain, which represents the ratio of the change in the control current for the change in the body current, can be calculated as equation (5).

$$A_I = \frac{\Delta I_B}{\Delta I_C} = r_m \cdot \frac{\Delta I_B}{\Delta V_O} = \frac{r_m}{R_B + R_L} \quad (5)$$

The calculated current gain is 0.8, which is almost the same value as 0.813 obtained from the waveforms of Fig. 6(a). As expected from equation (5), the current gain of SFFT is dependent on r_m, R_B and R_L.

The voltage gain, which describes the relation between the signal amplitude of the control line and the signal amplitude induced in the load terminal connecting with body line, can be derived as equation (6).

$$A_V = \frac{\Delta V_L}{\Delta V_C} = \frac{R_L}{R_B + R_L} \cdot r_m \cdot \frac{1}{R_C} \quad (6)$$

In case that V_{CC}, R_{CC} and I_B are 9 V, 1 kΩ and 15 mA respectively, the calculated voltage gain is 1.6. A large voltage gain can be achieved by decreasing R_C assuming $R_L >> R_B$. In case that I_B is 30 mA with the same values for V_{CC}, R_{CC} and I_B, the simulated waveforms for the voltage and current at the control line and the body line are shown in Fig. 6(b).

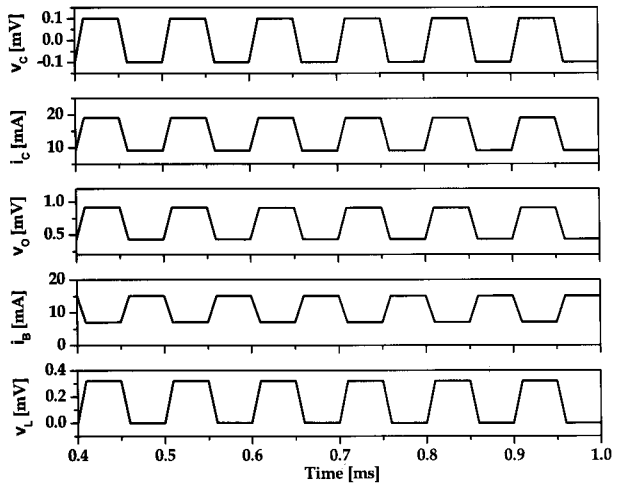

(a) V_{CC} = 9 V, R_{CC} = 1 kΩ, I_B = 15 mA

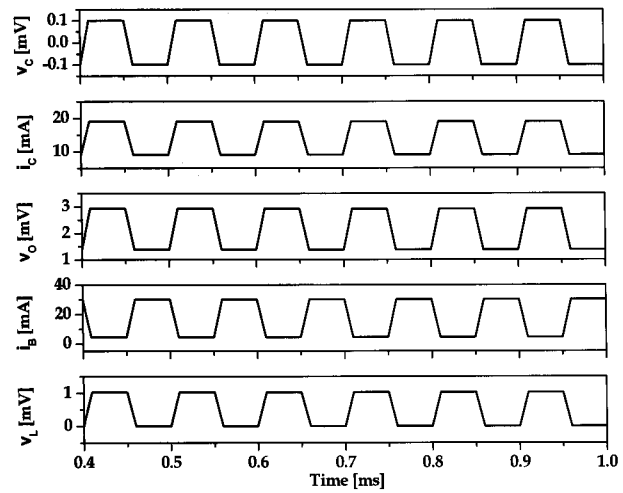

(b) V_{CC} = 9 V, R_{CC} = 1 kΩ, I_B = 30 mA

Fig. 6. The simulated waveforms for voltage and current at control line and body line.

The current and the voltage gains, which were calculated as 2.57 and 5.13 respectively, were more improved than the case of Fig. 6(a). The improvement of gain resulted from an increase of the transresistance, which was confirmed from Fig. 5. It was confirmed from this simulation that the current and the voltage gains of SFFT could be improved, although its transresistance is low.

4. CONCLUSIONS

We derived the voltage-current characteristics and the transresistance of SFFT considering the effect of magnetic field by the control current. From the equivalent circuit, which includes the transresistance of SFFT, the voltage and the current gains were drawn. By applying the numerical analysis for the equivalent circuit, the voltage and the current gains were estimated and compared with the calculated values. The methods to overcome the decrease of the gains due to low transresistance of SFFT were described. The research considering the mutual inductance including the self inductance of both the control line and the body line is required for the application of SFFTs into the various devices operating at the higher frequency.

ACKNOWLEDGMENT

This work was supported by the Soongsil University Research Fund.

REFERENCES

[1] K. Miyahara, S. Kubo, and M. Suzuki, "Vortex flow characteristics of high-Tc flux flow transistors", J. Appl. Phys., Vol. 75, No. 1, p. 404, 1994.

[2] J. S. Martens, T. E. Zipperian, V. M. Hietala, D. S. Ginley, C. P. Tigges, J. M. Phillips, and M. P. Siegal, "Superconducting flux flow digital circuits", IEEE Trans. Electron. Devices, Vol. 40, No. 3, p. 656, 1993.

[3] T. Bauch, S. Weiss, H. Haensel, A. Max, D. Koelle, and R. Gross, "High-temperature superconducting Josephson vortex flow transistors: numerical simulations and experimental results", IEEE Trans. Appl. Supercon., Vol. 7, No. 2, p. 3605, 1997.

[4] M. Pannetier, P. Bernstein, Ph. Lecoeur, O. Riou, T. D. Doan, and J. F. Hamet, "Determination of vortex motion characteristics, effective thickness and dynamic resistance in very thin YBaCuO bilayer

structures", IEEE Trans. on Appl. Supercon., Vol. 9, No. 2, p. 2635, 1999.
[5] E. Zeldov, N. M. Amer, G. Koren, A. Gupta, M. W. McElfresh, and R. J. Gambino, "Flux creep characteristics in high-temperature superconductors", Appl. Phys. Lett., Vol. 56, p. 680, 1990.
[6] T. Kiss, T. Nakamura, M. Takeo, K. Kuroda, Y. Matsumoto, and F. Irie, "Flux creep characteristics in the presence of a pinning distribution for $Y_1Ba_2Cu_3O_{7-\delta}$ superconducting thin films", IEEE Trans. on Appl. Supercon., Vol. 5, No. 2, p. 1363, 1995.
[7] H.-G. Kang, S.-C. Ko, M.-H. Choi, Y.-B. Hahn, and B.-S. Han, "Superconducting flux-flow transistor using plasma etching", J. of KIEEME(in Korean), Vol. 16, No. 5, p. 424, 2003.
[8] P. Bernstein, C. Picard, M. Pannetier, Ph. Lecoeur, J. F. Hamet, T. D. Doan, J. P. Contour, M. Drouet, and F. X. Reg, "Current-voltage characterization of the vortex motion in $YBa_2Cu_3O_{7-\delta}$ microbridges and implications on the development of superconducting flux flow transistor", J. Appl. Phys., Vol. 82, No. 10, p. 5030, 1997.